Int. J. Heat Mass Transfer. Vol. 34, No. 2, pp. 525–541, 1991
Printed in Great Britain

0017–9310/91 $3.00 + 0.00

Experimental study of free and mixed convection in horizontal porous layers locally heated from below

F. C. LAI and F. A. KULACKI
Department of Mechanical Engineering, Colorado State University, Fort Collins, CO 80523, U.S.A.

(*Received* 27 *April* 1989 *and in final form* 8 *April* 1990)

Abstract—Experimental results are reported for free and mixed convection in liquid saturated, horizontal porous layers with localized heating from below. Three different sizes of heat source have been considered which give a relative heater size (axial length/layer depth) of 1.0–5.0. For natural convection, Nusselt numbers have been obtained for Rayleigh numbers of practical interest, $1 \leqslant Ra_H \leqslant 1000$, while for mixed convection, results cover $1 \leqslant Ra_H \leqslant 1000$ and $0.1 \leqslant Pe_H \leqslant 120$. Based on dimensional analysis and non-linear regression, correlations for Nusselt number against Rayleigh and Peclet numbers have been obtained. Experimental Nusselt numbers compare very well with numerically calculated values. Improved agreement between calculations and measurements can be obtained through use of an effective thermal conductivity. The stability of the flow and temperature fields are also carefully examined. The existence of a Peclet number for which the overall heat transfer rate is a minimum is confirmed by experiment.

INTRODUCTION

HEAT TRANSFER in saturated porous media has recently received considerable attention because of its important applications in geophysics and energy-related engineering technologies. However, most existing fundamental studies have focused on natural convection, while few have been reported for mixed convection despite its equal importance in many situations. In addition, most studies have considered a uniformly heated lower boundary, while a finite, or local, heat source, which is encountered more frequently in practice, has received little attention. For natural convection in the non-uniformly heated case, Elder [1, 2] and Horne and O'Sullivan [3, 4] were the first to study buoyancy induced flows in horizontal layers with localized heating from below. Later, the problem was re-examined numerically by Prasad and Kulacki [5, 6]. However, no experimental results have been reported thus far.

For mixed convection, Wooding [7] made the first attempt to study combined free and forced convection in a porous layer, which later was followed by the studies of Prats [8], Sutton [9], and Homsy and Sherwood [10]. Using a boundary layer formulation and the similarity method, Cheng [11, 12] has conducted a series of investigations on mixed convection over vertical, inclined and horizontal plates. Recently, numerical results for mixed convection in horizontal and vertical porous layers with non-uniform heating on the boundary have been reported [13, 14]. Experimental work on mixed convection has been very limited and studies have been reported only by Combarnous and Bia [15], Fand and Phan [16], and Clarksean *et al.* [17].

The purpose of the present study is to experimentally examine the interactions between buoyancy and an externally induced flow over a horizontal surface which is locally heated. Experiments on natural convection are conducted first and the measured Nusselt numbers are then used as a limiting case for mixed convection. Heat transfer results are reduced to relations between Nusselt, Rayleigh and Peclet numbers for maximum utility in engineering design. The experimental results are also compared to those predicted by earlier numerical analysis [13, 18, 19] so as to validate the observed phenomena. Finally, some care has been taken in describing the experimental apparatus and procedure given the fundamental nature of the experiments. We hope this aspect of the paper will make the reduced data more useful for both applications to thermal engineering and future research.

EXPERIMENTAL APPARATUS

The apparatus has been carefully designed such that it has the capability of performing both natural and mixed convection experiments (Fig. 1). In addition, it requires minimum modifications when changing from one set of experiments to another. The major component is a long rectangular box made of Plexiglas. The box is divided into three sections by two sets of stainless steel screens. When conducting experiments for natural convection (Fig. 2(a)), these two screen sets are replaced by two Phenolite plates. In addition, three blocks of polystyrene insulation, each of 5.08 cm thick, are inserted to both entrance and exit sections to minimize heat losses. When performing mixed convection experiments (Fig. 2(b)), the entrance section is equipped with a flow distributor and a tube bundle which serves as a plenum to maintain a uniform flow in the test section. The entrance section also serves to collect any entrained air bubbles.

The exit section provides a return passage for the circulating water. Five thermocouple probes, 0.16 cm

NOMENCLATURE

c	specific heat of fluid at constant pressure [J kg^{-1} K^{-1}]
d	diameter of glass bead [m]
D	length of heat source [m]
Da	Darcy number, K/H^2
g	acceleration of gravity [m s^{-2}]
h	average heat transfer coefficient on the heated surface [W m^{-2} K^{-1}]
H	height of the porous layer [m]
k_e	effective thermal conductivity of the saturated porous medium [W m^{-1} K^{-1}]
k_m	stagnant thermal conductivity of the porous medium [W m^{-1} K^{-1}]
K	permeability of the saturated porous medium [m^2]
L	length of the porous layer [m]
Nu	average Nusselt number, hH/k
Pe	Peclet number, U_oH/α
q	uniform heat flux [W m^{-2}]
Ra	Rayleigh number, $Kg\beta qH^2/\nu\alpha k$
T	temperature [K]
U_o	uniform velocity of the external flow [m s^{-1}]
x, y	Cartesian coordinates [m].

Greek symbols

α	thermal diffusivity of porous medium, $k/(\rho c)_f$ [m^2 s^{-1}]
β	isobaric thermal expansion coefficient of fluid [K^{-1}]
ε	porosity
θ	dimensionless temperature
ν	kinematic viscosity of fluid [m^2 s^{-1}]
τ	dimensionless time
ω	weighting function, equation (3).

Superscript

*	quantity based on the mean temperature difference.

Subscripts

D	quantity based on the length of the heat source
e	quantity based on the effective thermal conductivity of the porous medium
f	fluid
H	quantity based on the height of the porous layer
m	quantity based on the stagnant thermal conductivity of the porous medium
w	condition at the wall
x	local variable
∞	condition at infinity.

in diameter, are mounted on the wall of this section. Three probes, each 45.72 cm long, are inserted in the test section at a height of 2.54 cm. They measure the temperature of the porous medium at three different locations, each 7.62 cm apart. Two probes 15.24 cm long are used to measure the temperature of exiting water.

The test section has a dimension of 1.067×0.305 m.

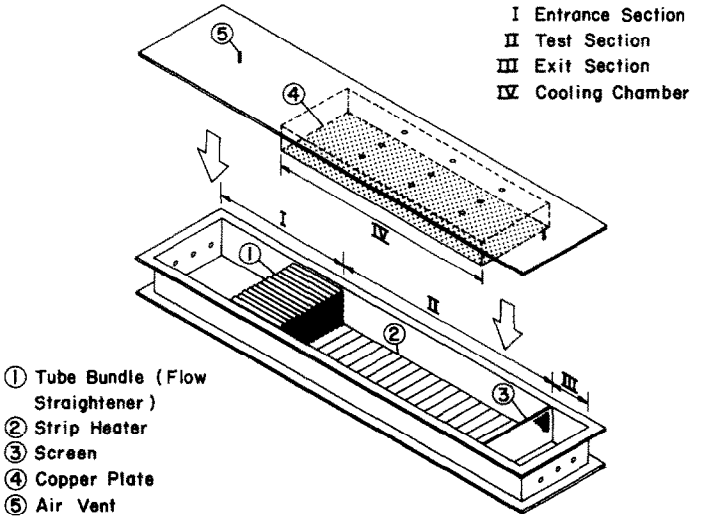

FIG. 1. Experimental apparatus used for the study of natural and mixed convection in a horizontal porous layer.

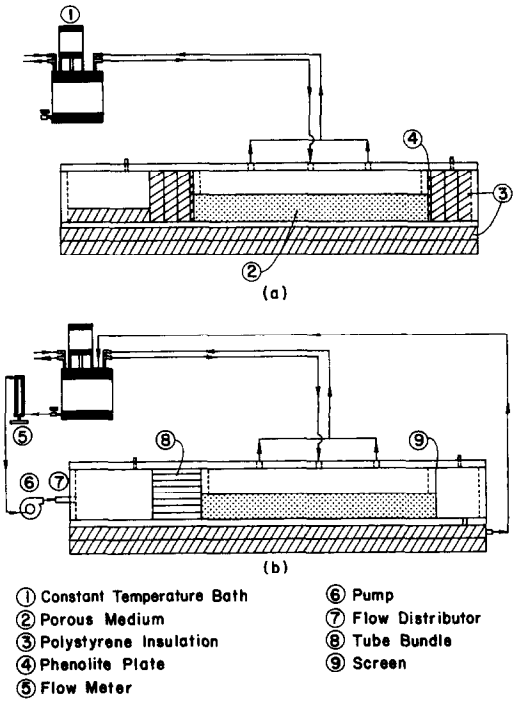

FIG. 2. Experimental set-up for the study of (a) natural convection and (b) mixed convection.

Twenty-one strip heaters are mounted on the bottom wall of this section. Each heater is 30.38 cm × 5.08 cm and is designed to provide a constant heat flux. Each of the heaters is individually controlled, and thus heat flux can be varied in segments along the length of the test section.

On the bottom wall of the test section, grooves are provided on both sides of the wall such that thermocouple wires can be set in and run through. Thus, the flatness of the test section can be ensured. Sixty-three thermocouples (30 Ga, type T) are then placed underneath the heaters with their junctions in direct contact with the heaters. Another 63 thermocouples of the same type are installed on the bottom surface in a 'one-on-one' correspondence. With this arrangement, each heater is monitored by at least six thermocouples, and heat loss in both lateral and longitudinal directions can therefore be accurately calculated.

Since the calculation of the average Nusselt number requires knowledge of the surface temperature of the heater, its accuracy therefore strongly depends on the precision of these measurements. An additional 20 thermocouples are attached to the surface of five heaters in the central portion of the test section. To minimize the interference to the flow field, fine gauge thermocouple wires (nominal size 0.56 mm × 0.96 mm) are used. By applying high temperature, highly conductive adhesive to the beads, the thermocouple junctions are attached to the heater surface. The beads are made as small as possible to minimize interference and provide accurate measurement and fast response. Four thermocouples are affixed to each heater, two in the center, and one at each end.

To effectively maintain an isothermally cooled top surface, a cooling chamber is provided (Fig. 1). The chamber is a rectangular box the bottom wall of which is a copper plate, while the rest of the walls are made of Plexiglas. Cooling water is circulated through the chamber from a thermostatically controlled source. Mixing and convective cooling is relied upon to maintain the copper plate at a constant temperature. Twelve thermocouples are mounted on the surface of the copper plate to monitor the temperature variation. When the input power to the heating elements on the lower surface is high, the flow rate of the cooling water is increased to maintain a constant temperature.

Two sheets of polystyrene insulations, each 5.08 cm thick are placed underneath the apparatus. The side walls are also insulated with three layers of polystyrene to a total thickness of 15.24 cm. These layers of insulation maintain nearly adiabatic thermal boundary conditions on the test section.

To minimize the errors which may otherwise arise due to an initial temperature difference between the incoming water and the cooling chamber, the circulating flows to the porous bed and the cooling chamber are drawn from the same constant temperature bath. In practice, because of the design of the apparatus and cooling chamber, small temperature fluctuations in the circulator reservoir produce only a negligible change in thermocouple readings from the incoming water and the copper plate of the cooling chamber. To accurately control the flow rate, a variable-speed pump has been used. A ten-turn speed control potentiometer with a latch to lock in settings is provided for a better control of the flow rate.

All thermocouples from the apparatus are connected to a data acquisition unit. All the thermocouple signals are directly converted to temperature readings by computer software.

EXPERIMENTAL PROCEDURE

Experiments were performed using 3 mm diameter glass beads and water as the saturated porous medium. The depth of the porous bed was kept constant at 5.08 cm, throughout the experiments. The porous layer under consideration thus had an aspect ratio of 21 : 1 and a packing parameter, d/H, of 0.059 (1/17). The reason for choosing such a long shallow bed is that the assumption of a two-dimensional flow is nearly met, and the effects of side walls can be minimized.

In the preparation of the experiments, the glass beads and the interior of the apparatus were carefully cleaned. The test section was then filled up to the desired height, 5.08 cm for the present study, with glass beads and water. To produce an isotropic and homogeneous porous medium, water and glass beads were added to the test section one by one. The appar-

atus was shaken gently to let the glass beads settle down nicely and release any trapped air. To avoid trapped air in the test section, water was added to a height of 2 cm over the porous bed. The cooling chamber was then placed in its position and was pushed down until it fully rested on the layer of glass beads, thus forcing excess water out of the entrance and exit sections. The apparatus was then entirely sealed. Before power was applied to the heaters, water from the constant temperature reservoir was circulated through both the cooling chamber and the apparatus for several hours so that the entire system would be at uniform temperature.

In all runs, sufficient time was allowed for the system to reach a steady state. To assure that the steady state had been reached, a strip chart recorder was used to monitor temperature variations at two locations. The time required to reach a steady state was dependent on Rayleigh number, Peclet number, and the size of the heat sources. In general, for higher Rayleigh numbers, less time was required to reach steady state. Data, namely thermocouple outputs, power inputs to heaters, and flow rates were recorded over a 10 min period at steady state. An average of five sets of readings comprised each data point reported here.

To minimize the experimental errors, heat losses from the apparatus were carefully identified and corrected before any correlations were developed. However, the Rayleigh, Peclet and Nusselt numbers presented in the final correlations are still subject to errors. These errors result from the uncertainties in the quantities used to calculate them. To perform an analysis on experimental errors, the uncertainties in the permeability and the effective thermal conductivity are unknown. These values are the subject of much heated debate in the literature and are often corrected in post experiment analysis. Therefore, the uncertainties in these quantities have been neglected in the error analysis, the confidence in the chosen correlations for these values stems from their successful use by many investigators.

To calculate the uncertainty in all the dimensionless groups, the law of summation of fractional errors is applied to give an estimate of the total fractional uncertainty. Based on this analysis, the estimated uncertainties for the Rayleigh, Peclet and Nusselt numbers are 4.7, 4.1 and 2.9%, respectively. The uncertainty in Peclet number is a maximum when the flow rate is a minimum. This is also true for Nusselt number, with the maximum uncertainty resulting from the smallest temperature difference.

For natural convection, experiments were conducted for a wide range of Rayleigh number and various sizes of heat source, i.e. $D/H = 1$, 3 and 5. For each size of heat source, the data were taken with the Rayleigh number (input power) being increased from low to high. For mixed convection, a full range of Peclet and Rayleigh numbers was explored. Thus, correlations could be determined from the given Peclet and Rayleigh numbers and the resulting Nusselt numbers. The range of the experimental data used to determine the final correlations are $0.1 \leqslant Pe_H \leqslant 120$ and $1 \leqslant Ra_H \leqslant 1000$. The Reynolds number based on the diameter of the glass bead is of the order of unity, which implies that inertial effects are negligible. In addition, the Darcy number for the present case is of the order of 10^{-5}, which further implies that Brinkman effects are insignificant [20]. Therefore, the applicability of Darcy's law in the present analysis is theoretically confirmed. Forced convection which becomes dominant when $Pe_H \geqslant 150$, is not considered here due to non-Darcy effects.

RESULTS

In the presentation of experimental results, the permeability used in the calculation of the Rayleigh number, Ra_H, is based on the Kozeny–Carman equation [21]

$$K = \frac{d^2\varepsilon^3}{180(1-\varepsilon)^2}. \quad (1)$$

Except for highly porous, fibrous, or fissured media, it has been reported that this equation gives a reasonable value of permeability [21, 22]. In the calculation of the Nusselt and Rayleigh numbers, the value of the effective thermal conductivity of a porous medium is required. In the present study, the mixture rule has been employed to the primary reduced values of Nusselt number and initial correlations for heat transfer. It has been reported that this conductivity model, although simple in form, gives very reasonable values of the stagnant thermal conductivity as long as there is no significant difference between k_s and k_f. We will return to the issue of how best to represent thermal conductivity later.

Natural convection

For a uniformly heated boundary, the criterion for the onset of natural convection in porous media has been well established. However, very little attention has been focused on the non-uniformly heated case. Therefore, the present study serves two purposes: (1) to provide experimental data for the validation of numerical solution of the governing partial differential equations, and (2) to provide results which later will be used as a limiting case in the study of mixed convection. Although we are without the aid of flow visualization, the flow field was carefully monitored through temperature recordings. Numerical results have also been used to get a better understanding of the convective heat transfer process. The numerical method and calculation procedure have been described in detail elsewhere [23, 24] and are omitted here for brevity.

When the porous layer is locally heated with a small flux, a weak convective cell is first generated at the edge of the heat source, due to the horizontal temperature gradient (Fig. 3(a)). For $D/H = 3$ and 5, it is observed that, for a large portion of domain over

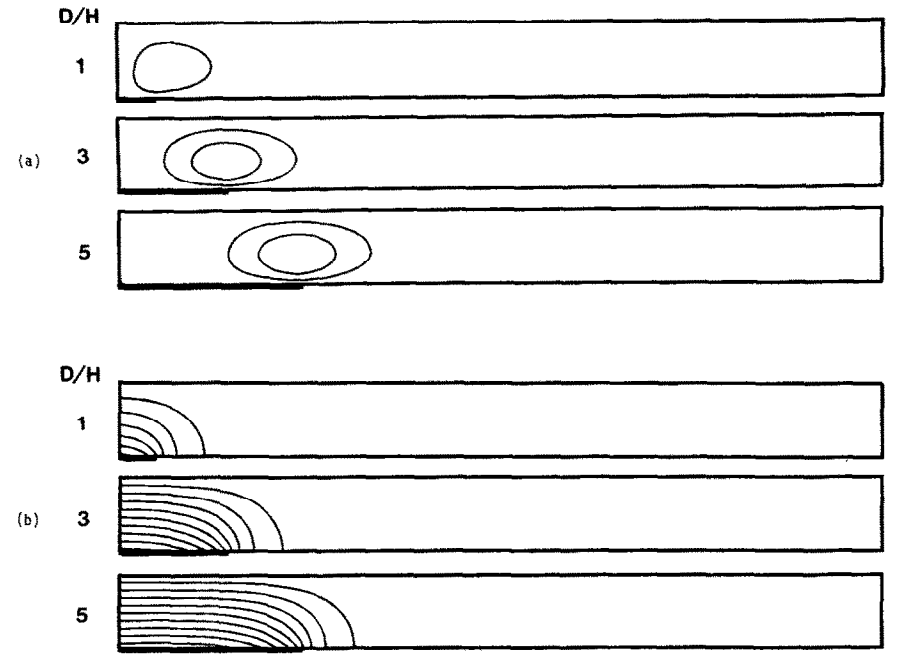

FIG. 3. Natural convection in a horizontal porous layer, for $Ra_H = 10$: (a) streamlines ($\Delta\psi = 0.1$) and (b) isotherms ($\Delta\theta = 0.1$).

the heat source, heat transfer is mainly by conduction (Fig. 3(b)). With an increase in the applied heat flux, the strength of the convective cells increases. For $D/H = 1$, it remains a single cell, while for $D/H = 3$ and 5, additional recirculating cells have formed in the layer (Fig. 4(a)). In the temperature field, a thermal plume is observed to rise from the heat source for $D/H = 1$, while for $D/H = 3$ and 5, ascending and descending plumes are found simultaneously (Fig. 4(b)).

When the flux is increased further such that the Rayleigh number is large, e.g. $Ra_H = 500$, it is interesting to see that for $D/H = 1$, the flow is unicellular, but for $D/H = 3$, the flow field has changed from

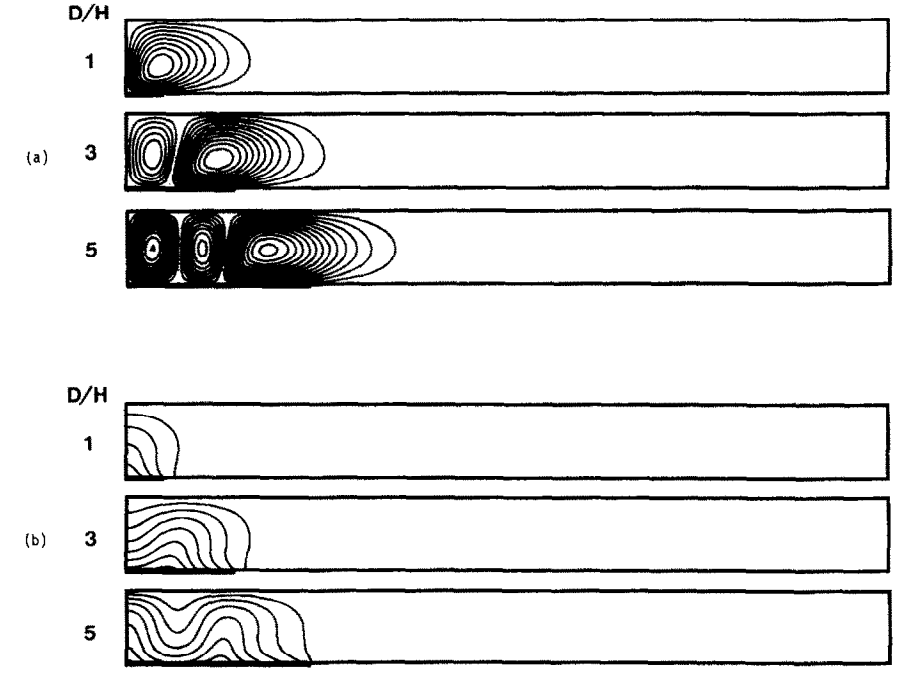

FIG. 4. Natural convection in a horizontal porous layer, for $Ra_H = 100$: (a) streamlines ($\Delta\psi = 0.2$) and (b) isotherms ($\Delta\theta = 0.1$).

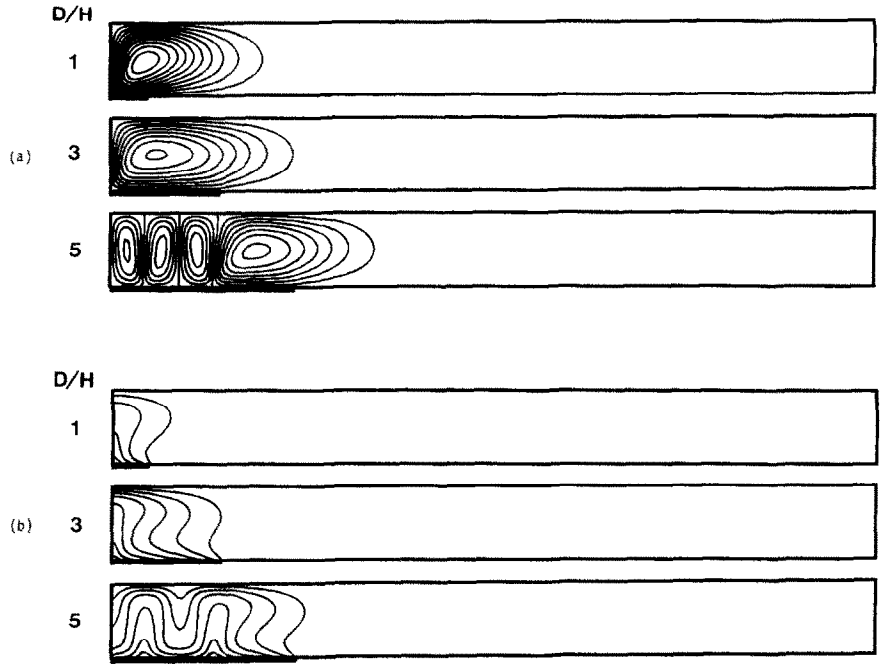

FIG. 5. Natural convection in a horizontal porous layer, for $Ra_H = 500$: (a) streamlines ($\Delta\psi = 1.0$) and (b) isotherms ($\Delta\theta = 0.05$).

multicellular to unicellular. For $D/H = 5$, an additional pair of cells has been generated in the field (Fig. 5). Even so, the flow fields remain stable which can be verified from the results of the transient study.

To obtain a better understanding of the transport process, the variation of the flow and temperature fields with time, for $D/H = 5$, are presented in Figs. 6 and 7, respectively. At small time, flow disturbance starts at the edge of the heat source and propagates toward the center, leaving the rest of the domain largely unaffected. Multiple cells are generated thereafter as long as the local Rayleigh number is above a critical value at which convection is initiated. Particular attention is drawn to the displacement of the

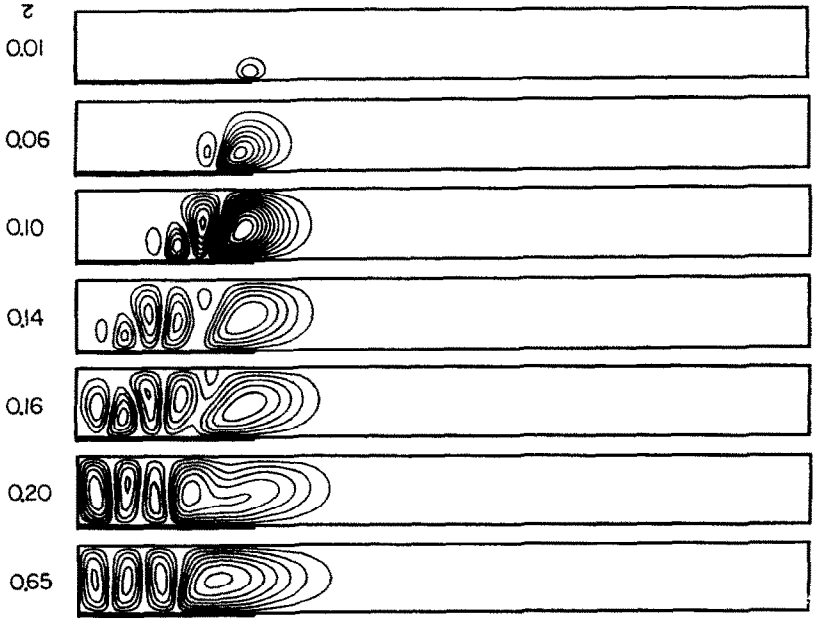

FIG. 6. Variation of flow field with time, for $D/H = 5$ and $Ra_H = 500$ ($\Delta\psi = 0.5$ for $\tau \leqslant 0.1$, $\Delta\psi = 1$ for $\tau > 0.1$).

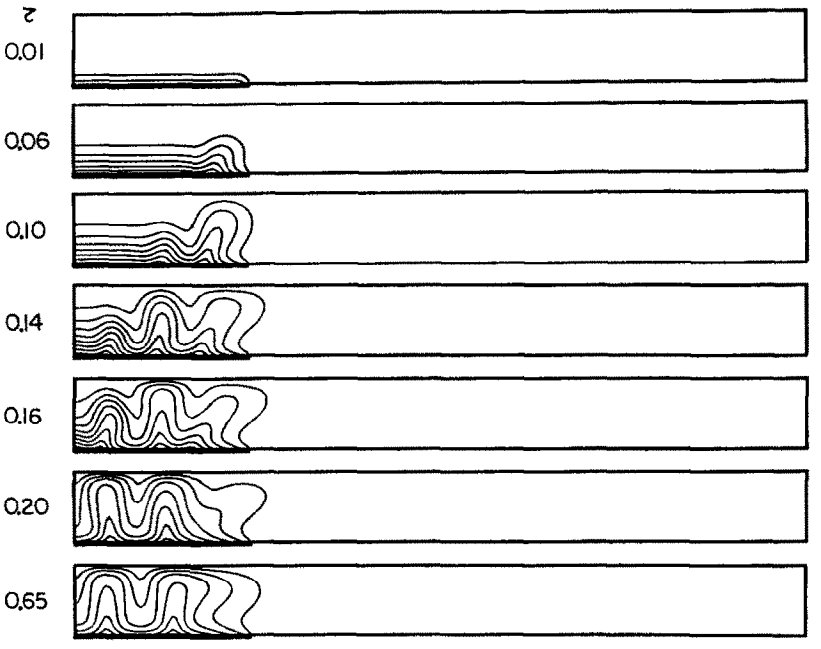

FIG. 7. Variation of temperature field with time, for $D/H = 5$ and $Ra_H = 500$ ($\Delta\theta = 0.05$).

streamlines as a disturbance is generated. Finally, a steady state is reached after all the small disturbances are dissipated through the unheated domain.

The present results differ from those of Horne and O'Sullivan [3, 4] in that no flow (temperature) oscillation has been observed. However, Horne and O'Sullivan [3] studied the case of a square cavity. In that case, the disturbance, once generated, is not totally dissipated through the unheated region. In turn, it triggers the appearance of the next disturbance, which leads the flow field to an oscillatory state. For the present case and that studied by Prasad and Kulacki [5, 6], the geometry considered is a rectangular cavity with the aspect ratio of 10.5 and 5, respectively. Thus, the additional unheated region provides an access to dissipate the disturbances, and hence weakens the triggering mechanism to the flow instability.

The above observation made from the numerical study can be verified by the experimental results. The temperature variation on the heated surface which was recorded in the experiments is compared with the numerical solution in Fig. 8. The experimental data selected for the comparison have a Rayleigh number close to the numerical values. In general, the agreement between these two results are very good. Especially, the nice agreement at $Ra_H = 100$ for $D/H = 3$ and 5, has further confirmed the multicellular convection observed in the numerical study.

Heat transfer results in terms of average Nusselt number on the heated wall are presented in Fig. 9 for $D/H = 1$, 3 and 5. As reported by Nield [25] as well as Ribando and Torrance [26], the flow field is less stable when it is heated from below with a constant flux than by a constant temperature bottom wall. For a fully heated bottom wall, the critical Rayleigh number for the constant flux case is found to be 27.1, instead of 40 ($4\pi^2$) for the isothermal case. Due to the non-uniform heating, it is noticed that convection starts at an even lower Rayleigh number. At a lower Rayleigh number, the present results agree well with the numerical results. However, as the Rayleigh number increases, the experimental data are lower than the numerical predictions for $D/H = 1$, while they are higher for $D/H = 3$ and 5. Nonetheless, both results show the same trend. The maximum difference between the experimental and numerical results is about 20%, but mostly they are within 10% of the numerical values.

Mixed convection

When an external flow is introduced to a porous layer which is locally heated from below, the resulting flow and temperature field can be quite different from the no-flow condition, i.e. free convection case. Depending on the introduced flow rate, the flow and temperature field can be characterized as the free, mixed and forced convection regime.

When the external flow rate is small, the flow and temperature fields retain the characteristics of natural convection. The symmetry of the streamline and isotherm patterns (Fig. 10) clearly shows the domination of buoyancy. However, for $D/H = 3$, the flow field has changed from a multicellular structure (Fig. 4(a), for free convection) to a bicellular one due to the introduction of the external flow.

An increase in the external flow rate weakens the buoyancy effect, while it increases the forced convection effects. This is clearly seen from the destruc-

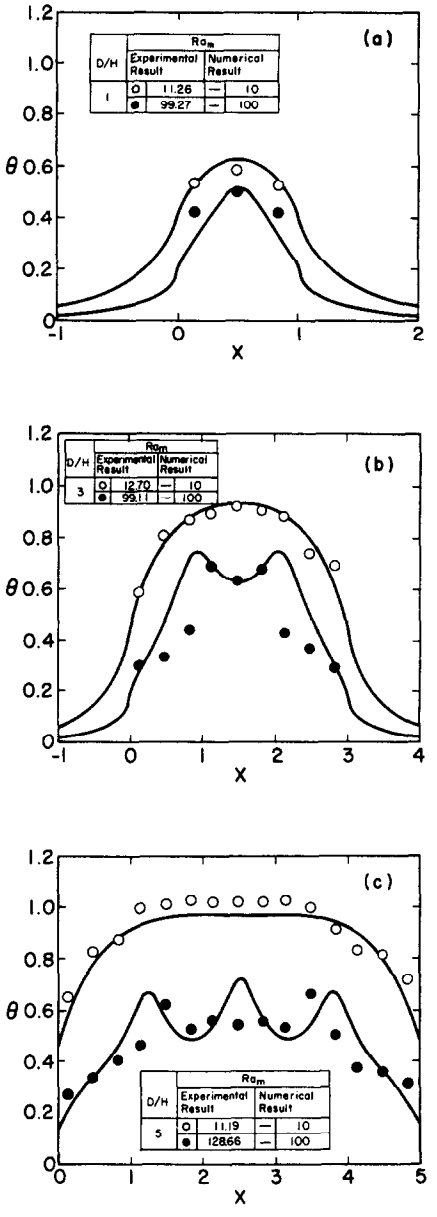

FIG. 8. Temperature distribution on the heated surface: (a) $D/H = 1$; (b) $D/H = 3$; (c) $D/H = 5$.

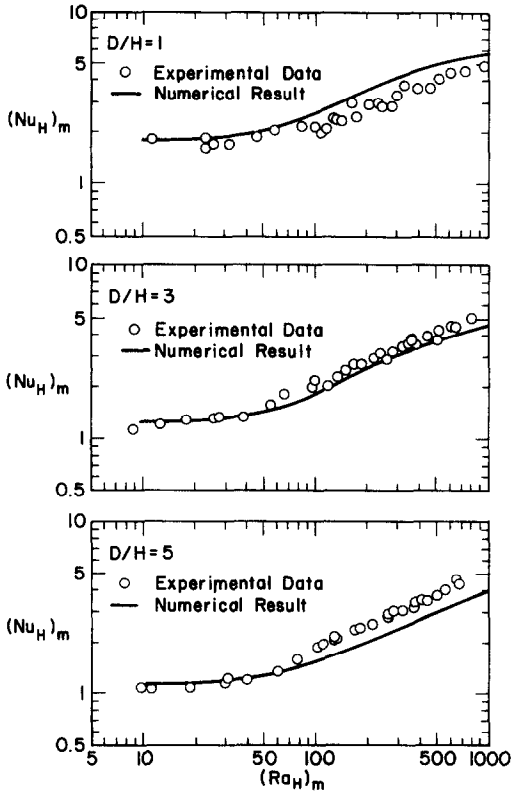

FIG. 9. Average Nusselt number based on stagnant thermal conductivity and layer height (natural convection).

tion of the symmetry of streamline and isotherm patterns (Fig. 11). In addition, it is noted that for $D/H = 5$, the flow becomes oscillatory. The flow oscillation observed in the present case is very similar to what has been previously reported [18, 19]. If the external flow rate is increased further, the forced convection effects become dominant, while the buoyancy effects are diminished (Fig. 12). It is very interesting to see that the flow field for $D/H = 5$ becomes stable again. The cause of the instability will be elaborated on further in the following sections.

To closely examine the interaction between the buoyancy effects and the forced flow, a series of experiments have been conducted. First, to show the important role that the buoyancy effects play in the mixed convection, the external flow rate was kept constant while the input power was increased accordingly. The results of this set of experiments are presented in Fig. 13. It is clearly seen that the buoyancy effects are dominant at a low Peclet number and become negligible at a high Peclet number.

On the other hand, to see forced convection effects, the input power was set constant while the external flow rate was varied. Figure 14 contains the results of this set of experiments. The data of the corresponding natural convection cases are also shown in the figure. It is clearly observed that at a small Peclet number, the heat transfer results for mixed convection are about the same as those for natural convection, which indicates the domination of the buoyancy effects at a small Peclet number. When the Peclet number increases, the contribution to the total heat transfer by forced convection increases, while the contribution by natural convection is decreased due to the diminishing effects of buoyancy. The result of this balance is the existence of a Peclet number, for which the total heat transfer is a minimum. As the Peclet number is increased further, the enhancement of heat transfer by forced convection becomes more evident. The results shown here thus validate prior numerical studies [13, 18].

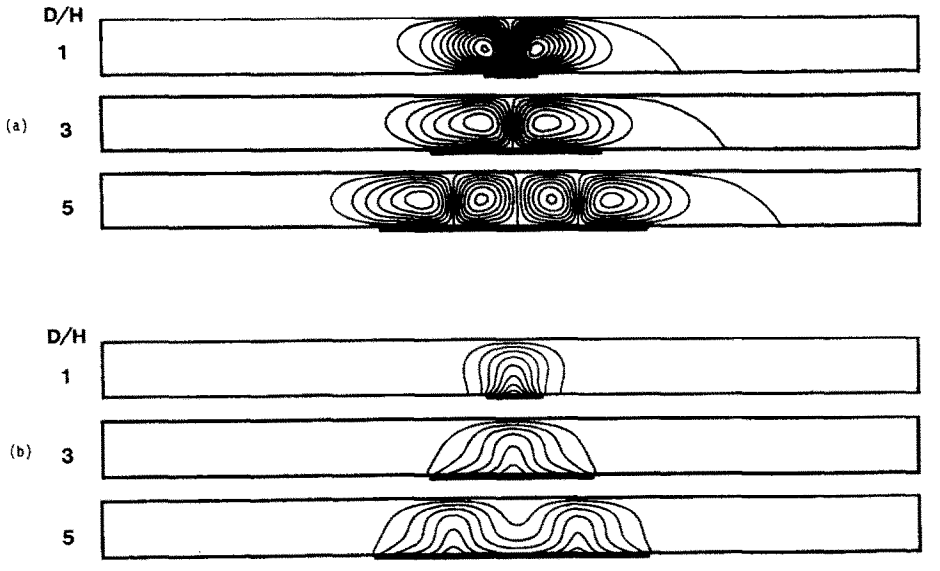

FIG. 10. Mixed convection in a horizontal porous layer, for $Ra = 100$ and $Pe = 0.1$: (a) streamlines ($\Delta\psi = 1$ for $D/H = 1$, $\Delta\psi = 2$ for $D/H = 3, 5$) and (b) isotherms ($\Delta\theta = 0.1$).

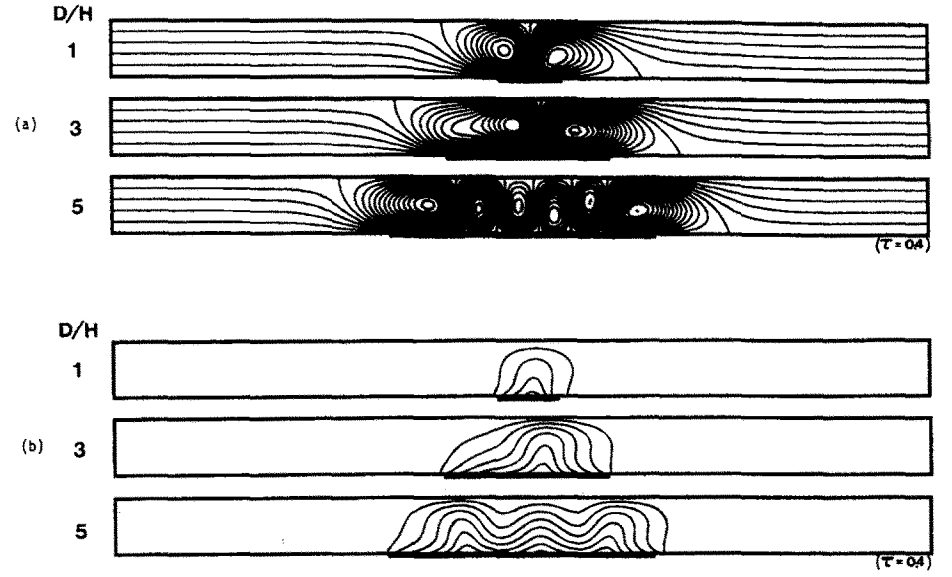

FIG. 11. Mixed convection in a horizontal porous layer, for $Ra = 100$ and $Pe = 1$: (a) streamlines ($\Delta\psi = 0.2$) and (b) isotherms ($\Delta\theta = 0.1$).

It is interesting to point out that the oscillatory behavior in the flow field reported from the numerical study [18, 19] has also been observed in the experiments. Figure 15 shows the variation of the surface temperature with time. For free convection, the origin of oscillatory convection in a porous medium has been studied by Horne and O'Sullivan [3, 4]. They concluded that the disturbances result from a combination of cyclic triggering by their predecessors that circulated around the convective cells and the instability of the thermal boundary layer. However, in the present case, the disturbance was convected downstream due to the external flow, which minimizes the triggering of thermal disturbances by their circulating predecessors. Therefore, it can be concluded that the only mechanism for oscillatory convection is due to the instability of the thermal boundary layer. This instability, in turn, is due to the interaction between the forced flow and buoyancy effects. While buoyancy effects tend to thicken the thermal boundary layer, forced flow suppresses it. With the existence of the upper wall, this interaction has been further inten-

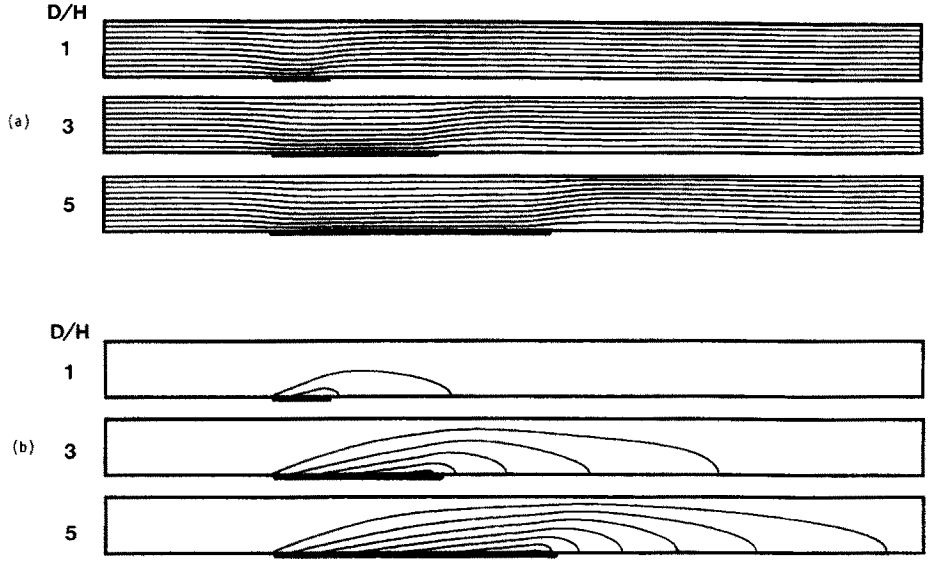

FIG. 12. Mixed convection in a horizontal porous layer, for $Ra = 100$ and $Pe = 10$: (a) streamlines ($\Delta\psi = 0.1$) and (b) isotherms ($\Delta\theta = 0.1$).

sified. The destruction and regeneration of circulating cells observed in the previous study [19] is the result of this process. The above argument can be verified by examining the time variation of the isotherm patterns [19].

Heat transfer results for mixed convection can be best presented in terms of two governing parameters, $Nu/Pe^{1/2}$ and $Ra/Pe^{3/2}$ (Fig. 16). As observed in the natural convection case, the experimental data are lower than the numerical prediction for $D/H = 1$, while they are higher for $D/H = 5$. Again, the maximum difference between the experimental and numerical results is about 20%, but mostly they are well within 10%. Nevertheless, these two results show the same trend.

Effective thermal conductivity

The observed discrepancy between the measured and predicted Nusselt number in the above results is very similar to what has been reported in many studies when a thermal conductivity of the saturated medium is either based on a measured stagnant (i.e. no change) value or calculated via some mixture rule. Various theories have been proposed to explain this. Among them, use of an 'effective' thermal conductivity [23, 24, 27] seems most reasonable and will be employed to improve the agreement between the experimental and numerical results. What is proposed is that the thermal conductivity in the energy equation is not the stagnant thermal conductivity (i.e. based on the mixture rule) but the conductivity of the medium when the fluid is flowing. Since the fraction of energy transported by the fluid increases with convection, the effective thermal conductivity is expected to change and approach that of the fluid as the Rayleigh number increases. This concept was simply expressed [24, 27] by viewing the conductivity to comprise a component which depended on the convective state of the fluid, i.e. on Rayleigh number. Thus

$$k_e = \omega k_f + (1-\omega)k_m \tag{2}$$

where

$$\omega = 1 - \frac{Nu_{\text{conduction}}}{Nu_m}. \tag{3}$$

As is clear from equation (3), the weighting function ω is based on the fraction of energy transferred by the fluid due to convection, and will increase as the convective flow increases. Hence, the effective thermal conductivity k_e equals k_m for pure conduction and asymptotically approaches k_f as the convective component increases. Whether the purely convective limit can be reached awaits conclusive experimental proof, but in diagnosis from the present and earlier experiments [23, 27], however, are encouraging. The variation of the weighting function is shown in Fig. 17 as a function of the Rayleigh number. As proposed, it increases with the Rayleigh number and approaches an asymptotic value when the Rayleigh number becomes large.

Heat transfer correlations

For natural convection, the correlation of heat transfer results based on the original experimental data is given by

$$Nu_D = 0.269 Ra_D^{0.451}, \quad Ra_D \geqslant 40 \tag{4}$$

and for the corrected data

$$Nu_D = 0.516 Ra_D^{0.357}, \quad Ra_D \geqslant 40. \tag{5}$$

Based on the numerical results, the correlation is

$$Nu_D = 0.520 Ra_D^{0.354}, \quad Ra_D \geqslant 40. \tag{6}$$

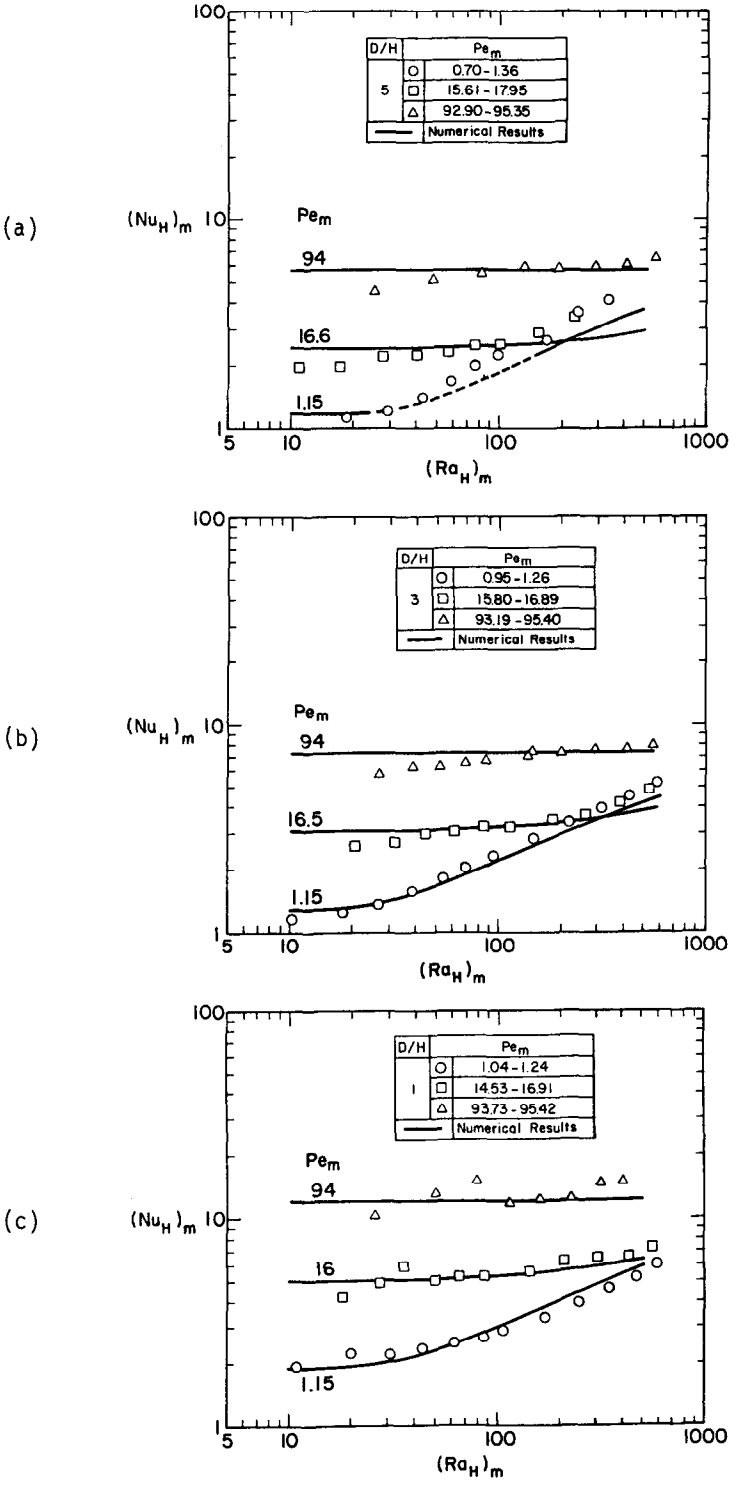

FIG. 13. Experimental results for buoyancy effects on mixed convection in a horizontal porous layer: (a) $D/H = 1$; (b) $D/H = 3$; (c) $D/H = 5$.

As noticed, the last two correlations agree with each other very well. It has been reported that for natural convection over a horizontal surface embedded in a saturated porous medium, similarity solutions exist for the case of constant surface heat flux [28]. The average Nusselt number in this case is given by

$$Nu_D = 1.402 Ra_D^{*1/3}. \quad (7)$$

It should be noted that the Rayleigh number in equation (7) is defined based on the mean temperature

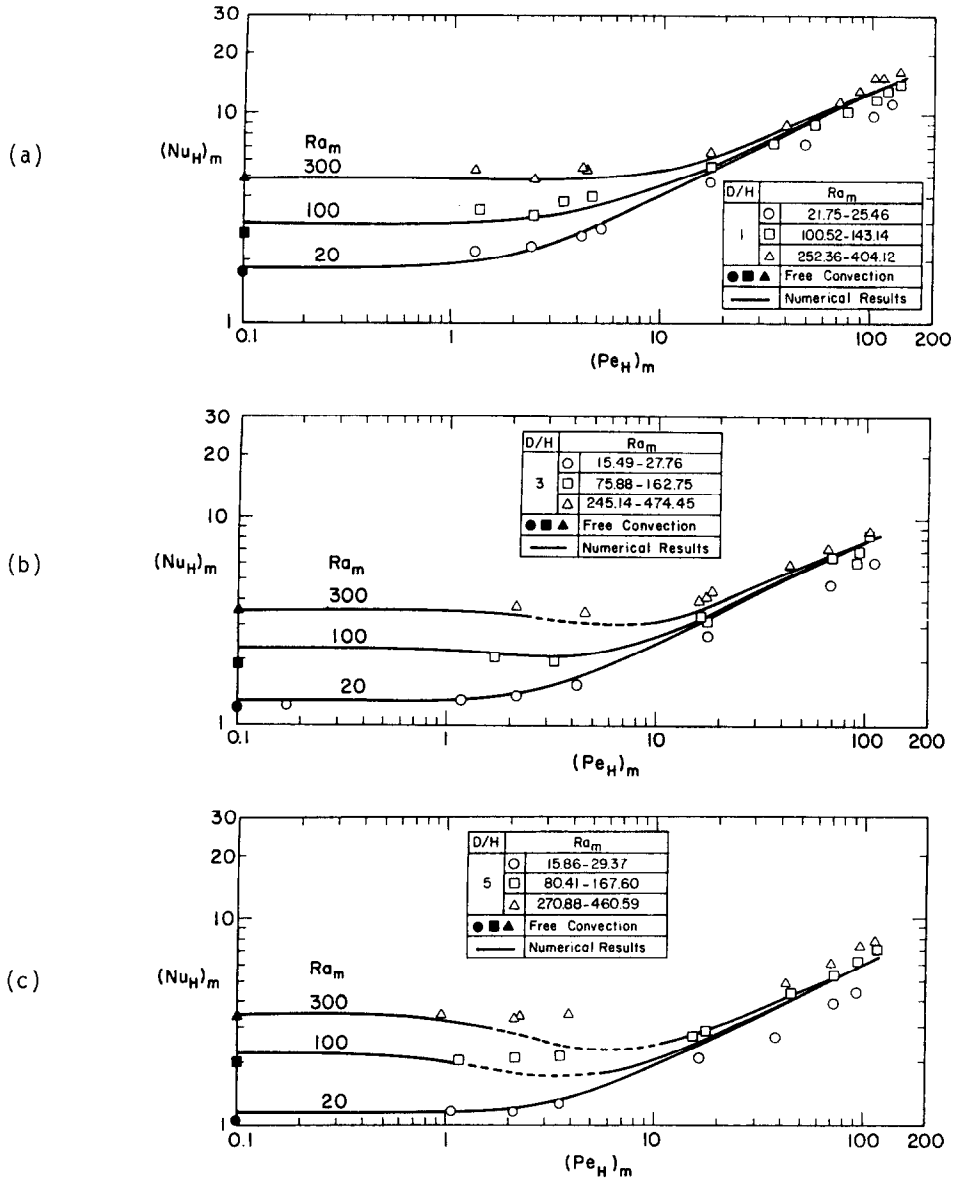

FIG. 14. Experimental results for effects of forced flow on mixed convection in a horizontal porous layer: (a) $D/H = 1$; (b) $D/H = 3$; (c) $D/H = 5$.

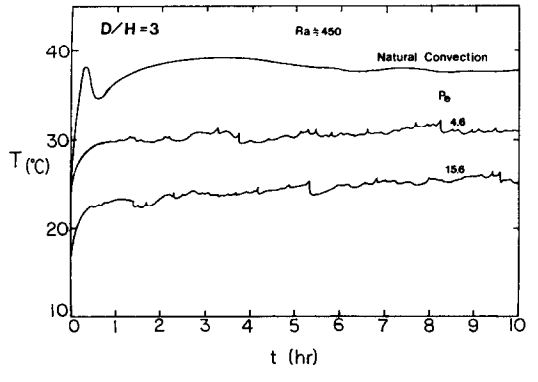

FIG. 15. Variation of surface temperature with time (mixed convection).

difference on the heated wall, i.e. $Ra_D^* = Kg\beta(T_w - T_\infty)D/\nu\alpha$. For comparison, it can also be defined based on the applied heat flux, i.e. $Ra_D = Kg\beta qD^2/k\nu\alpha$, and the relation is given by

$$Ra_D^* = \frac{Ra_D}{Nu_D}. \tag{8}$$

In this case, equation (7) can be rewritten as

$$Nu_D = 1.288 Ra_D^{1/4}. \tag{9}$$

It is important to note that the power of the Rayleigh number has changed from 1/3 (based on the mean temperature difference) to 1/4 (based on the applied heat flux). Equations (5) and (9) are plotted in Fig. 18 for comparison. It is noticed that the pre-

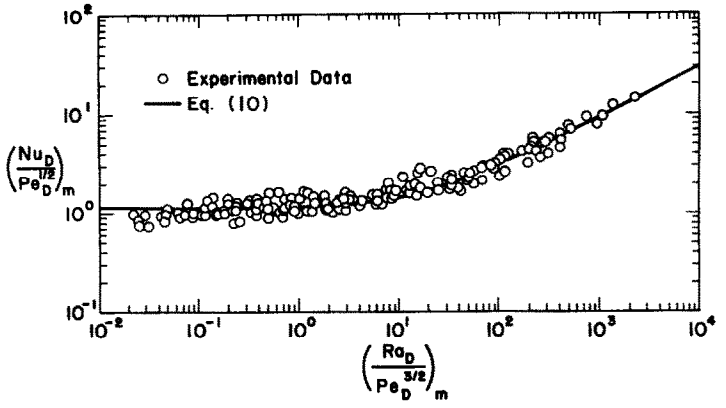

FIG. 16. Heat transfer results based on stagnant thermal conductivity (mixed convection).

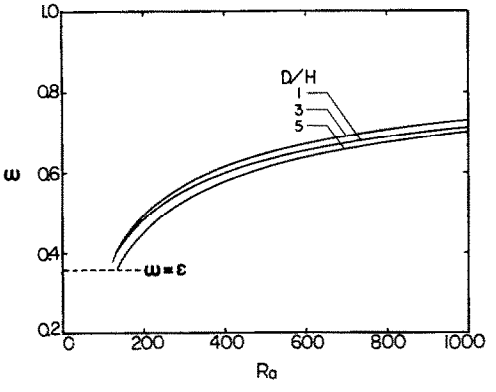

FIG. 17. Variation of weighting function, ω, with Rayleigh number (natural convection).

diction by the similarity solution is fairly good at high Rayleigh numbers, which can be expected since the boundary-layer approximations used in the formulation are valid only at a high Rayleigh number. However, it is also noticed that the similarity solution underpredicts the result at a higher Rayleigh number, e.g. $Ra_D \geqslant 6000$. This is due to the breakdown of the boundary-layer assumption since the boundary layer cannot grow indefinitely in the presence of the upper wall. Nevertheless, the similarity solution can be safely used as a lower bound on the heat transfer rate at a higher Rayleigh number.

For mixed convection, when the experimental data are presented in terms of the Nusselt, Rayleigh and Peclet numbers which are based on the effective thermal conductivity, a much better agreement is also found with the numerical prediction (Fig. 19). The results are best correlated by the following empirical formula:

$$\frac{Nu_D}{Pe_D^{1/2}} = \left[1.274 + 0.079\left(\frac{Ra_D}{Pe_D^{3/2}}\right)\right]^{0.506}$$

for original data (10)

$$\frac{Nu_D}{Pe_D^{1/2}} = \left[1.895 + 0.200\left(\frac{Ra_D}{Pe_D^{3/2}}\right)\right]^{0.375}$$

for corrected data (11)

and

$$\frac{Nu_D}{Pe_D^{1/2}} = \left[1.917 + 0.210\left(\frac{Ra_D}{Pe_D^{3/2}}\right)\right]^{0.372}$$

for numerical results. (12)

As presented by Cheng [12], similarity solutions exist for mixed convection over a horizontal surface embedded in a saturated porous medium. The heat

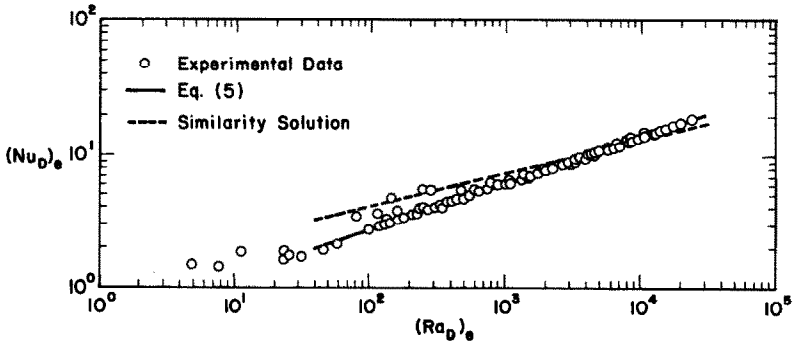

FIG. 18. Average Nusselt number based on effective thermal conductivity (natural convection).

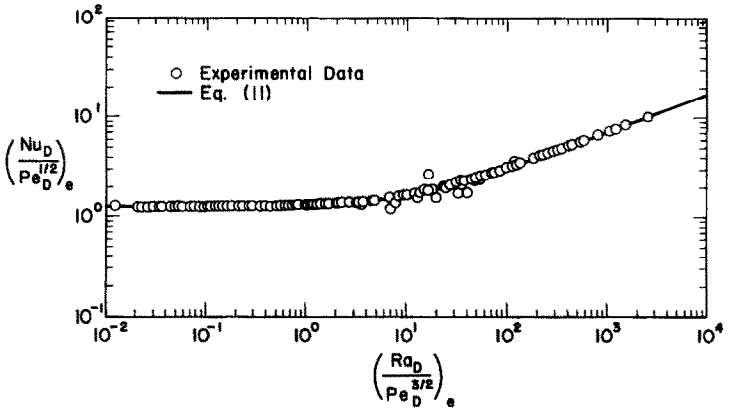

FIG. 19. Heat transfer results based on effective thermal conductivity (mixed convection).

transfer result in terms of the governing parameter $Nu/Pe^{1/2}$ is given by

$$\frac{Nu_x}{Pe_x^{1/2}} = -\theta'(0) \tag{13}$$

where $-\theta'(0)$, which is the non-dimensional heat flux at the wall, is a function of $Ra_x/Pe_x^{3/2}$. It is noted, however, that the governing parameters in equation (13) are defined based on the local coordinate, i.e. $Nu_x = hx/k$, $Ra_x = Kg\beta(T_w - T_\infty)x/\nu\alpha$ and $Pe_x = U_\infty x/\alpha$. If they were defined based on the heated length, then the numerical values of equation (13) can be correlated by

$$\frac{Nu_D^*}{Pe_D^{1/2}} = \left[2.598 + 2.769\left(\frac{Ra_D^*}{Pe_D^{3/2}}\right)\right]^{1/3}. \tag{14}$$

Again, it should be noted that the Rayleigh number in equation (14) is defined based on the mean temperature difference on the heated surface. For comparison, it can be expressed in terms of the applied heat flux and the heat transfer results can thus be correlated by

$$\frac{Nu_D}{Pe_D^{1/2}} = \left[3.111 + 3.039\left(\frac{Ra_D}{Pe_D^{3/2}}\right)\right]^{1/4}. \tag{15}$$

It is noticed that the power of the correlation has also changed from 1/3 to 1/4, which is consistent with the natural convection results. Table 1 summarizes the correlation formulae that have been proposed in the present study, along with their estimated errors.

It is interesting to point out that the Peclet number, at which the total heat transfer rate is a minimum, does not exist for mixed convective flow over a horizontal surface embedded in a semi-infinite porous medium (i.e. similarity solution). This can be verified by taking the derivative of Nusselt number with respect to Peclet number, either from equation (14) or (15). This shows that the minimum Nusselt number occurs at $Pe = 0$. Thus, introducing any flow, no matter how small it may be, will always enhance the heat transfer rate. For the present case, this kind of relationship is not found.

To estimate the Peclet number of minimal heat transfer in the present case, the Nusselt number in equation (11) is differentiated with respect to the Peclet number, which gives

$$(Pe_D)_{\min} = 0.054 Ra_D^{2/3} \tag{16}$$

or

$$(Pe_H)_{\min} = 0.054\left(\frac{D}{H}\right)^{1/3} Ra_H^{2/3}. \tag{17}$$

It should be noted that the Peclet number thus

Table 1. Correlations for free and mixed convection in horizontal porous layers

	Correlation	Standard error
Similarity solution	Free convection $Nu_D = 1.288 Ra_D^{1/4}$	—
	Mixed convection $Nu_D/Pe_D^{1/2} = [3.111 + 3.039(Ra_D/Pe_D^2)]^{1/4}$	0.081
Numerical results	Free convection $Nu_D = 0.520 Ra_D^{0.354}$	0.327
	Mixed convection $Nu_D/Pe_D^{1/2} = [1.917 + 0.210(Ra_D/Pe_D^{3/2})]^{0.372}$	0.641
Experimental	Free convection $(Nu_D)_m = 0.269(Ra_D)_m^{0.451}$	0.637
	$(Nu_D)_c = 0.516(Ra_D)^{0.357}$	0.430
	Mixed convection $(Nu_D/Pe_D^{1/2})_m = [1.274 + 0.079(Ra_D/Pe_D^{3/2})_m]^{0.506}$	2.934
	$(Nu_D/Pe_D^{1/2})_c = [1.895 + 0.200(Ra_D/Pe_D^{3/2})_c]^{0.375}$	0.987

Standard error: $\sqrt{(\Sigma_n (Nu_{exp} - Nu_{cal})^2/n)}$ where Nu_{exp} is the Nusselt number obtained by the experiments or numerical study and Nu_{cal} the Nusselt number predicted by the given correlation.

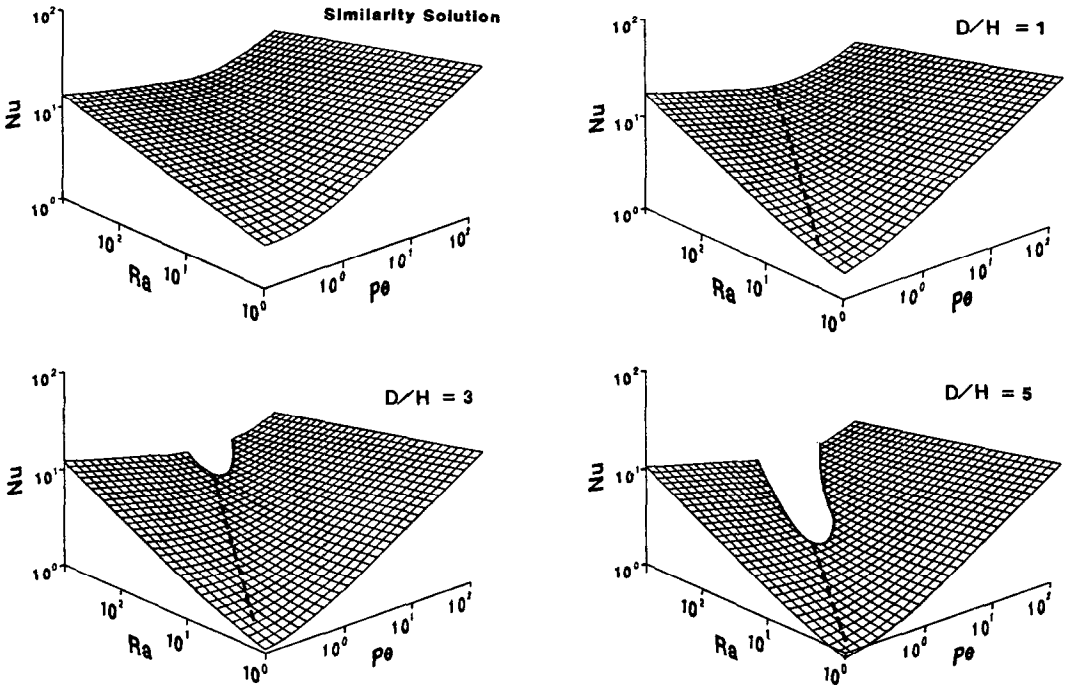

FIG. 20. Three-dimensional presentation of heat transfer results for mixed convection in a horizontal porous layer.

obtained is only an estimate and is subject to the same order of accuracy as the correlation formula from which it was derived. It clearly shows that the derived Peclet number is a function of the Rayleigh number, and for a fixed Rayleigh number (based on the height of the porous layer), it increases with the size of heat source. These observations have been confirmed by both numerical and experimental results.

The present results can be best visualized by a three-dimensional plot which shows the relation among the Nusselt, Rayleigh and Peclet numbers (Fig. 20). For better understanding and completeness, the Peclet number of minimal heat transfer and the oscillatory flow regime are plotted in the same figure. While the Peclet number curve is given by equation (17), the oscillatory flow regime is estimated from the numerical and experimental results. It is clearly shown that, for a fixed Rayleigh number, the Peclet number for minimal heat transfer increases with the heated length. In addition, the regime of flow instability also increases with the size of the heat source. For $D/H = 3$ and 5, it is found that for a high Rayleigh number, the location of the Peclet number of minimal heat transfer is always in the oscillatory flow regime. These observations are in good agreement with what has been discussed earlier.

CONCLUSIONS

Experiments have been conducted to study free and mixed convection in horizontal porous layers. When the experimental data are presented in terms of the Nusselt, Rayleigh and Peclet number based on the stagnant thermal conductivity of the porous medium, the experimental data are found to be smaller than those predicted by numerical results for $D/H = 1$, and larger for $D/H = 3$ and 5. The maximum difference between these two results is observed to be about 20%, but it is mostly within 10%. Despite some experimental scatter, the data show a similar trend that is predicted by the numerical results. A reasonable explanation for the scattering of experimental data in the highly convective regime is due to the inappropriate presentation of the thermal conductivity of the saturated medium. By employing the effective thermal conductivity model, the experimental data are in excellent agreement with the numerical results.

For natural convection, the oscillation in the flow and temperature field, which has been reported by Elder [1, 2] and Horne and O'Sullivan [3, 4], was not observed in the present study. This is due to the additional unheated region provided in the present case, which serves as a buffer zone to dissipate the small disturbances generated in the flow field such that the 'triggering' mechanism to the flow instability is greatly weakened. However, for mixed convection, the oscillation in the flow and temperature field does exist in the experiments and numerical study. It is due to the instability of the thermal boundary layer as a result of the strong interaction between the buoyancy effects and the forced flow.

For free convection, it is found that the results can be best correlated by Nu and Ra, while for mixed convection, $Nu/Pe^{1/2}$ and $Ra/Pe^{3/2}$. The power in the

correlation formula depends on how the governing parameters were defined. When the Rayleigh number is defined based on the applied heat flux, the power is 0.354 for natural convection and 0.372 for mixed convection. The results have also been compared with similarity solutions. It shows that these two results are in good agreement when the boundary-layer approximation holds.

Acknowledgement—The support of this work by the U.S. Nuclear Regulatory Commission and the Computer Center and the Colorado State University is greatly appreciated.

REFERENCES

1. J. W. Elder, Steady free convection in a porous medium heated from below, *J. Fluid Mech.* **27,** 29–48 (1967).
2. J. W. Elder, Transient convection in a porous medium, *J. Fluid Mech.* **27,** 609–623 (1967).
3. R. N. Horne and M. J. O'Sullivan, Oscillatory convection in a porous medium heated from below, *J. Fluid Mech.* **66,** 339–352 (1974).
4. R. N. Horne and M. J. O'Sullivan, Origin of oscillatory convection in a porous medium heated from below, *Physics Fluids* **21,** 1260–1264 (1978).
5. V. Prasad and F. A. Kulacki, Natural convection in horizontal porous layers with localized heating from below. In *Heat Transfer in Porous Media and Particulate Flows* (Edited by L. S. Yao *et al.*), HTD-Vol. 46, pp. 199–208. American Society of Mechanical Engineers, New York (1985).
6. V. Prasad and F. A. Kulacki, Effects of the size of heat source on natural convection in horizontal porous layers heated from below, *Proc. 8th Int. Heat Transfer Conf.*, pp. 2677–2682. Hemisphere, New York (1986).
7. R. A. Wooding, Convection in a saturated porous medium at large Rayleigh number or Peclet number, *J. Fluids Mech.* **15,** 527–544 (1963).
8. M. Prats, The effect of horizontal fluid flow on thermally induced convection currents in porous medium, *J. Geophys. Res.* **71,** 4835–4837 (1966).
9. F. M. Sutton, Onset of convection in a porous channel with net through flow, *Physics Fluids* **13,** 1931–1934 (1970).
10. G. M. Homsy and A. E. Sherwood, Convective instabilities in porous media with through flow, *A.I.Ch.E. Jl* **22,** 168–174 (1976).
11. P. Cheng, Combined free and forced convection flow about inclined surfaces in porous media, *Int. J. Heat Mass Transfer* **20,** 807–814 (1977).
12. P. Cheng, Similarity solutions for mixed convection from horizontal impermeable surfaces in saturated porous media, *Int. J. Heat Mass Transfer* **20,** 893–898 (1977).
13. V. Prasad, F. C. Lai and F. A. Kulacki, Mixed convection in horizontal porous layers heated from below, *J. Heat Transfer* **110,** 395–402 (1988).
14. F. C. Lai, V. Prasad and F. A. Kulacki, Aiding and opposing mixed convection in a vertical porous layer with a finite wall heat source, *Int. J. Heat Mass Transfer* **31,** 1049–1061 (1988).
15. M. A. Combarnous and P. Bia, Combined free and forced convection in porous media, *Soc. Petrol. Engrs J.* **11,** 399–405 (1971).
16. R. M. Fand and R. T. Phan, Combined forced and natural convection heat transfer from a horizontal cylinder embedded in a porous medium, *Int. J. Heat Mass Transfer* **30,** 1351–1358 (1987).
17. R. Clarksean, N. Kwendakwema and R. Boehm, A study of mixed convection in a porous medium between vertical concentric cylinders, *Proc. 1988 Natn. Heat Transfer Conf.*, Houston, Vol. 2, pp. 339–344 (1988).
18. F. C. Lai, V. Prasad and F. A. Kulacki, Effects of the size of heat source on mixed convection in horizontal porous layers heated from below, *Proc. 2nd ASME/JSME Thermal Engng Joint Conf.*, Honolulu, Vol. 2, pp. 413–419 (1987).
19. F. C. Lai and F. A. Kulacki, Transient mixed convection in horizontal porous layers partially heated from below, *Proc. 1988 Natn. Heat Transfer Conf.*, Houston, Vol. 2, pp. 353–364 (1988).
20. B. K. G. Chan, C. M. Ivey and J. M. Barry, Natural convection in enclosed porous media with rectangular boundaries, *J. Heat Transfer* **92,** 21–27 (1970).
21. J. Bear, *Dynamics of Fluids in Porous Media.* Elsevier, New York (1972).
22. A. E. Scheidegger, *The Physics of Flow through Porous Media.* University of Toronto Press, Toronto (1974).
23. V. Prasad, Natural convection in porous media—an experimental and numerical study for vertical annular and rectangular enclosures, Ph.D. Dissertation, University of Delaware (1983).
24. F. C. Lai, Free and mixed convection in porous media, Ph.D. Dissertation, University of Delaware (1988).
25. D. A. Nield, Onset of thermohaline convection in a porous media, *Water Resour. Res.* **14,** 553–560 (1968).
26. R. I. Ribando and K. E. Torrance, Natural convection in porous medium: effects of confinement, variable permeability and thermal boundary conditions, *J. Heat Transfer* **98,** 42–48 (1976).
27. V. Prasad, F. A. Kulacki and M. Keyhani, Natural convection in porous media, *J. Fluid Mech.* **150,** 89–119 (1985).
28. P. Cheng and I. Chang, Buoyancy induced flow in a saturated porous medium adjacent to impermeable horizontal surface, *Int. J. Heat Mass Transfer* **19,** 1267–1272 (1976).

ETUDE EXPERIMENTALE DE LA CONVECTION NATURELLE ET MIXTE DANS UNE COUCHE POREUSE HORIZONTALE AVEC CHAUFFAGE PAR LE BAS ET LOCALISE

Résumé—On présente des résultats sur la convection naturelle et mixte dans des couches poreuses horizontales saturées de liquide, avec un chauffage localisé à la base. On a considéré différentes tailles de source thermique qui donne des rapports longueur axiale/épaisseur de la couche entre 1,0 et 5,0. Pour la convection naturelle, les nombres de Nusselt sont obtenus avec des nombres de Rayleigh d'intérêt pratique, $1 \leqslant Ra_H \leqslant 1000$, tandis que pour la convection mixte les résultats couvrent le domaine $1 \leqslant Ra_H \leqslant 1000$ et $0{,}1 \leqslant Pe_H \leqslant 120$. A partir de l'analyse dimensionnelle et d'une régression linéaire, des formules sont obtenues pour le nombre de Nusselt en fonction des nombres de Rayleigh et de Peclet. Les nombres de Nusselt calculés s'accordent bien avec les valeurs expérimentales. Une amélioration de l'accord peut être obtenue en utilisant une conductivité thermique effective. La stabilité des champs de vitesse et de température est examinée avec soin. L'expérience confirme l'existence d'un nombre de Peclet pour lequel le flux de chaleur global est minimal.

EXPERIMENTELLE UNTERSUCHUNG DER FREIEN UND DER MISCH-KONVEKTION IN EINER WAAGERECHTEN, PORÖSEN, ÖRTLICH VON UNTEN BEHEIZTEN SCHICHT

Zusammenfassung—Es werden Versuchsergebnisse für die freie und die Misch-Konvektion in einer flüssigkeitsgesättigten, waagerechten, porösen, örtlich von unten beheizten Schicht vorgestellt. Dabei werden 3 unterschiedlich große Wärmequellen betrachtet, denen relative Heizflächenparameter (axiale Länge/Schichtdicke) von 1–5 entsprechen. Für natürliche Konvektion wurden Nusselt-Zahlen bei Rayleigh-Zahlen im praktisch interessierenden Bereich ($1 \leqslant Ra_H \leqslant 1000$) ermittelt, für Misch-Konvektion erstrecken sich die Versuche in folgenden Bereichen: $1 \leqslant Ra_H \leqslant 1000$ und $0{,}1 \leqslant Pe_H \leqslant 120$. Mittels Dimensionsanalyse und nichtlinearer Regression ergeben sich Korrelationen zwischen Nusselt-Zahl, Rayleigh-Zahl und Peclet-Zahl. Die experimentell bestimmten Nusselt-Zahlen stimmen gut mit numerisch berechneten Werten überein. Diese Übereinstimmung kann noch verbessert werden, wenn eine effektive Wärmeleitfähigkeit verwendet wird. Die Stabilität des Strömungs- und des Temperaturfeldes wird ebenfalls sorgfältig untersucht. Die Existenz einer Peclet-Zahl, bei der der Gesamtwärmedurchgang ein Minimum erreicht, wird durch das Experiment bestätigt.

ЭКСПЕРИМЕНТАЛЬНОЕ ИССЛЕДОВАНИЕ СВОБОДНОЙ И СМЕШАННОЙ КОНВЕКЦИИ В ГОРИЗОНТАЛЬНЫХ ПОРИСТЫХ СЛОЯХ ПРИ ЛОКАЛЬНОМ НАГРЕВЕ СНИЗУ

Аннотация—Экспериментально исследуется свободная и смешанная конвекция в насыщенных жидкостью горизонтальных пористых слоях при локализованном нагреве снизу. Рассмотрены три различных размера источника тепла с относительным размером нагревателя (осевая длина/глубина слоя), изменяющимся в диапазоне 1,0–5,0. В случае естественной конвекции значения числа Нуссельта определены для представляющих практический интерес значений числа Рэлея $1 \leqslant Ra_H \leqslant 1000$; в случае же смешанной конвекции результаты охватывают диапазон $1 \leqslant Ra_H \leqslant 1000$ и $0{,}1 \leqslant Pe_H \leqslant 120$. На основе анализа размерностей и нелинейной регрессии получены зависимости числа Нуссельта от чисел Рэлея и Пекле. Экспериментальные значения числа Нуссельта очень хорошо согласуются с расчетными значениями. Согласие между расчетами и измерениями может быть улучшено посредством использования эффективной теплопроводности. Также изучается устойчивость полей течения и температур. Экспериментально подтверждается существование значения числа Пекле, при котором скорость суммарного теплопереноса минимальна.